Available online at https://jcst.rsu.ac.th
Formerly Rangsit Journal of Arts and Sciences (RJAS)

Journal of Current Science and Technology, July-December 2020 JCST Vol. 10 No. 2, pp. 183-194

ISSN 2630-0656 (Online)

In silico and *in vitro* analysis of the role of cowaxanthone as a histone deacetylase inhibitor and apoptosis inducer in human leukemic T-cells

Sakdiphong Punpai[1], Audchara Saenkham[2], Kiattawee Choowongkomon[3], Sunit Suksamrarn[2], and Wanlaya Tanechpongtamb[1*]

[1]Department of Biochemistry, Faculty of Medicine, Srinakharinwirot University, Bangkok 10110, Thailand
[2]Department of Chemistry and Center of Excellence for Innovation in Chemistry, Faculty of Science, Srinakharinwirot University, Bangkok 10110, Thailand
[3]Department of Biochemistry, Faculty of Science, Kasetsart University, Bangkok 10903, Thailand

*Corresponding author; E-mail: wanlaya@g.swu.ac.th

Received 25 May 2020; Revised 30 June 2020; Accepted 15 July 2020
Published online 22 July 2020

Abstract

Histone deacetylase inhibitors (HDACis) are a class of anticancer agents that have received great attention. There are several of these compounds that are already being used in the clinical phase. However, unwanted side effects to patients are still illustrated. In this study, we aimed to discover a new type of HDACi from a natural agent. A natural xanthone, cowaxanthone, isolated from *Garcinia fusca* Pierre was selected due to its potential effects on cancer cytotoxicity. *In silico* docking and *in vitro* screening activity assays were carried out in order to investigate its role as an HDACi. The cytotoxic effects were also determined by MTT assay against Jurkat and MDA-MB-231 cells and compared to normal Vero cells. In addition, the mode of apoptotic death was preliminarily detected. As a result, cowaxanthone showed an optimum scoring function (docking energy) on all chosen target HDACs in class I (HDACs 2 and 8) and II (HDACs 4 and 7) with binding energies of 105.56, 74.24, 81.00 and 92.88 kcal/mol, respectively. These scores were high and in a similar range to those of standard HDACis, trichostatin A (TSA) and vorinostat (SAHA). In addition, cowaxanthone inhibited HDAC activity *in vitro* in a dose-dependent manner, in which increasing levels of acetylation of histones H3 and H4 were observed. The anticancer effects of cowaxanthone were clearly indicated in both Jurkat and MDA-MB-231 cells, which less toxic to Vero cells. Moreover, DNA fragmentation, apoptotic bodies and caspase-3, caspase-8 and caspase-9 activation were indicated. In conclusion, our results revealed a novel role of cowaxanthone as an HDACi, in which both classes I and II are inhibited. Apoptotic death was also suggested to be the cowaxanthone cytotoxicity mechanism.

Keywords**:** *apoptosis, cowaxanthone, Garcinia fusca Pierre, HDAC, histone deacetylase inhibitor, in silico docking*

1. Introduction

Histone deacetylases (HDACs) are an enzyme family that catalyzes the cleavage of acetyl groups from lysine residues of histone proteins and various nonhistone proteins. There are four distinct classes identified in humans according to their described structure. Members of HDAC class I are HDACs 1, 2, 3, and 8; class II are HDACs 4, 5, 6, 7, 9 and 10; class III are sirtuins named as SIRT1-7; and class IV contains only HDAC 11. HDAC classes I, II and IV are regarded as the classical HDAC enzyme families and share similar catalytic pocket sites that use Zn^{2+} as a cofactor, whereas HDAC class III enzymes (SIRTs) use nicotinamide adenine dinucleotide (NAD^{+}) as a cofactor (de Ruijter, van Gennip, Caron, Kemp, & van Kuilenburg, 2003). The activity of HDACs is well known to be a crucial regulator of gene transcription. Removal of acetyl groups results in a compact chromatin configuration that restricts transcription factor access to DNA and represses gene expression. HDAC function is the opposite of that of histone acetyl transferases (HATs), which catalyze histone acetylation, the activity of which leads to a less condensed DNA structure and increased gene transcription. These epigenetic regulations are critical to various cellular processes, such as cell proliferation, cell cycle progression, and cell death. The dysregulation of both HDACs and HATs plays a part in the development of several diseases. For carcinogenesis, evidence has shown that imbalances in both HDACs and HATs often occur. The expression of HDACs is markedly increased in various human cancers, such as ovarian, liver, lung, breast, cervical, colorectal and hematological tumors (Singh, Bishayee, & Pandey,

2018). Thus, inhibition of HDACs is considered a promising way to reduce cancer progression.

Currently, a range of histone deacetylase inhibitors (HDACis) have been identified as a new class of anticancer agents from both natural and synthetic sources. HDACis potentially induce differentiation, cell cycle arrest and apoptosis in cancer cells (Zhang & Zhong, 2014). This apoptotic process is a crucial target mechanism because it does not elicit an inflammatory response in the surrounding cells. Two main pathways have been illustrated, extrinsic or death receptor-mediated and intrinsic or mitochondria-mediated. Both pathways are mainly regulated by activation of the caspase family of enzymes. Caspase-8 and caspase-9 are the initiator caspases of the extrinsic and intrinsic pathways, respectively. Caspase-3 is the major executioner caspase that induces DNA fragmentation and causes cell death (Jan & Chaudhry, 2019). Most HDACis have been demonstrated to be involved in the activation of both extrinsic and intrinsic signaling and have been accepted as potential anticancer agents. Currently, several of HDACis have been approved by the US Food and Drug Administration (FDA) for use in the clinic, such as vorinostat (SAHA), belinostat and romidepsin (Yoon & Eom, 2016). However, unwanted side effects to patients from HDACis are still present, so new potential agents from natural sources are needed to add more options for treatment.

Cowaxanthone is a natural xanthone compound (structure shown in Figure 1) that was isolated from a few *Garcinia* plants, including *Garcinia fusca* Pierre (family Clusiaceae), which is distributed in several Southeast Asian countries. In Thailand, *G. fusca* is known as Madan-Paa or Mak-Mong (Nontakham, Charoenram, Upamai, Taweechotipatr, & Suksamrarn, 2014). The fruits and leaves are edible, and the leaves are used to relieve cough and fever. The major chemical components isolated from *G. fusca* were xanthones and bioflavonoids, which are well known as important sources that can be applied in the clinic. Xanthone compounds obtained from *G. fusca* include cowanol, cowanin, β-mangostin, α-mangostin, cowaxanthone, fuscaxanthone, rubraxanthone, norcowanin, isojacareubin, garbogiol and 7-O-methylgarcinone (Nguyen et al., 2017). Most of these compounds have been explored in pharmacological aspects, and various bioactivities have been observed, such as anticancer, antioxidant, antimicrobial, antiviral, and antifungal activities (Negi, Bisht, Singh, Rawat, & Joshi, 2013). However, the bioactivity of cowaxanthone has not yet been investigated. The cytotoxicity of cowaxanthone against cancer cells has only been described in breast, lung, oral and colon cancer cell lines (Ha et al., 2009). Additionally, its mechanism of inducing cancer cell death is still in the preliminary stages, and the role of HDACis has not yet been investigated.

2. Objectives

In the current study, we aimed to investigate a new type of HDACi from xanthone that is potentially cytotoxic to cancer cells. A computational tool, *in silico* docking analysis, was selected to determine the possibility of the HDAC inhibition functions of cowaxanthone following an *in vitro* study. Cytotoxicity against cancer cells was also assessed in leukemic T cells (Jurkat cells) and breast cancer cells (MDA-MB-231). The levels of cytotoxicity were compared with African green monkey kidney cells (Vero), a representative normal cell line. Furthermore, a preliminary investigation of the mechanism of apoptotic cell death induction was evaluated.

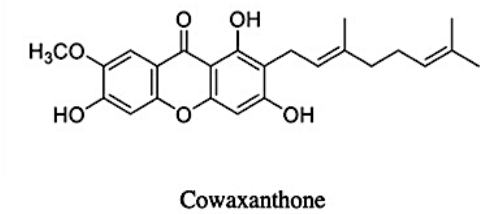

Cowaxanthone

Figure 1 The chemical structure of cowaxanthone extracted from the plant *Garcinia fusca*

3. Materials and methods

3.1 Reagents

RPMI 1640 (Roswell Park Memorial Institute 1640) medium, DMEM (Dulbecco's modified Eagle's medium), MEM (minimum essential medium), fetal bovine serum (FBS) and penicillin-streptomycin were obtained from GIBCO (Invitrogen, USA). Thiazolyl blue tetrazolium bromide (MTT) was obtained from USB Corporation, USA. A histone deacetylase assay kit (CS1010) was obtained from Sigma-Aldrich, USA. Hoechst 33342 fluorescent solution was obtained from Invitrogen, USA.

3.2 Compound isolation and characterization

Cowaxanthone was isolated from *G. fusca* as previously described (Nontakham et al., 2014). In brief, the chopped dried root of *G. fusca* (1 kg) was thoroughly extracted with ethyl acetate at 50°C. The EtOAc soluble fraction was evaporated to dryness (40 g) and subjected to column chromatography over silica gel eluting with a gradient of hexane-acetone to yield 18 main fractions. Cowaxanthone was obtained as a yellow solid (49 mg) from a silica gel column (eluting with a gradient of hexane-acetone) in fraction 7. The NMR data of cowaxanthone were consistent with the reported values, and its purity exceeded 97% as shown by HPLC.

3.3 Cell culture

Human leukemic T-cells (Jurkat cells, clone E6-1), human breast cancer cells (MDA-MB-231) and African green monkey kidney cells (Vero) were obtained from the American Type Culture Collection (ATCC, USA). Jurkat, MDA-MB-231 and Vero cells were cultured in RPMI 1640, DMEM and MEM, respectively. All media contained 10% (v/v) heat-inactivated fetal bovine serum (FBS), 100 mM HEPES, 100 mM sodium pyruvate, 100 U/mL penicillin, and 100 µg/mL streptomycin (Gibco, USA). All cell types were cultured in a humidified atmosphere at 5% CO_2 and 37°C. Cells in the log phase were used in the experiments.

3.4 *In silico* docking analysis

In order to predict the interactions between cowaxanthone and HDAC classes I and II, *in silico* docking was performed. The 3D crystal structures of target human HDAC2, HDAC4, HDAC7 and HDAC8 (PDB codes: 3MAX, 2VQM, 3C10 and 1T64, respectively) were downloaded from the PDB (Berger et al., 2013). Then, self-docking of each HDAC was performed to confirm the structure and method. After that, the 3D structures of the cowaxanthone ligand and the positive HDAC inhibitors, trichostatin A (TSA) and vorinostat (SAHA), were downloaded from the PubChem compound database (CID: cowaxanthone = 10386850, TSA = 444732 and SAHA= 5311) and docked with all 4 target HDACs into each catalytic pocket using GOLD version 5.3.0 (Cambridge, UK). The 2D molecular interaction models were analyzed by Discovery Studio 2017 R2 client software (Cambridge, UK) and UCSF Chimera (California, USA).

3.5 HDAC inhibitor screening assay

The screening of HDAC inhibitor activity was determined according to the kit protocol supplied by the manufacturer (Sigma-Aldrich, MO, USA). Briefly, cowaxanthone was mixed with Jurkat cell lysates as a source for HDAC activity in the inhibitor screening assay. Then, the sample reactions were added to a substrate containing a fluorescent group followed by developer solution. After incubation for 10 min, release of the free highly fluorescent product was measured using a Synergy™ HT multi-mode microplate reader (Bio-Tek Instruments, USA) with an excitation wavelength of 360 nm and emission wavelength of 460 nm. The measured fluorescence was directly proportional to the activity of each sample. TSA and SAHA were used as positive controls, whereas DMSO was used as a negative control.

3.6 Cell viability assay

To determine the cytotoxic effects of cowaxanthone, an MTT assay was conducted in different cell lines. Jurkat, MDA-MB-231 and Vero cells were chosen and seeded at a density of 50,000, 10,000, and 20,000 cells/well in 96-well plates, respectively. Then, various concentrations of cowaxanthone (0-100 µM; 2-fold dilution) were added in triplicate, while the control group was treated with 0.5% DMSO. After 24 h of incubation, 5 mg/mL MTT solution (final concentration of 0.5 mg/mL) was added to each well and incubated for 2 h at 37°C. Then, the insoluble purple formazan crystal products were dissolved in DMSO and quantified by measuring the color intensity at a wavelength of 570 nm using a microplate reader (Bio-Tek Instruments, USA). The inhibitory concentration at 50 % (IC_{50}) was calculated using

GraphPad Prism 5.03 software (GraphPad Software, Inc., San Diego, CA, USA).

3.7 Apoptotic nuclear morphology determination

Jurkat cells were treated with different concentrations of cowaxanthone (0, 60, 80 and 100 μM) for 24 h. Then, the cells were stained with 5 μg/mL Hoechst 33342 (Invitrogen, USA), a DNA-specific fluorescent dye, for 30 min. Then, the nuclear morphology was observed under an Olympus reflected fluorescence microscope (IX73; Olympus, Tokyo, Japan).

3.8 Western blot analysis of caspases and histone acetylation

Activation of caspase-3, caspase-8 and caspase-9 and hyperacetylation of histones H3 and H4 were analyzed by Western blot analysis. Cells were cultured in six-well plates at 1×10^6 cells per well and then treated with cowaxanthone at 0, 60, 80 or 100 μM for 12 h. After that, the samples were lysed with RIPA solution for 60 min on ice. Cell suspensions were centrifuged at 15,000 rpm for 30 min. Then, a final concentration of 40 μg/mL protein extracts was separated by SDS-PAGE, and proteins were transferred onto PVDF membranes (Bio-Rad Laboratories, USA). Next, the resulting blots were subjected to immunodetection with the primary antibody at 1:1000 and subsequently with the corresponding secondary antibody. The membranes were detected by the ECL reagent (Sigma-Aldrich, Germany) and visualized with a UVITEC chemiluminescence imaging system (UVITEC Limited, Cambridge, UK).

3.9 Statistical analysis

The results were analyzed and are expressed as the mean ± standard deviation of three independent experiments. Statistical analysis was performed using one-way ANOVA followed by Dunnett's multiple-comparison test using GraphPad Prism version 5.0 (San Diego, USA), and *p*-values of $*p<0.05$, $**p<0.01$ and $***p<0.001$ were considered statistically significant.

4. Results and discussion

4.1 Computational *in silico* docking analysis indicates the role of cowaxanthone as an HDACi

Over past decades, *in silico* docking analysis has been extended and broadly applied to drug discovery and development processes, especially target identification and validation. Therefore, as we aimed to discover a new type of anticancer agent from a natural source that potentially targets HDAC enzymes, we selected this interesting tool to predict the possibility before further investigation with an *in vitro* study. The natural compound xanthone, cowaxanthone, was selected for investigation. This was because natural xanthones are well accepted as a group of compounds that exhibit various bioactivities (Negi et al., 2013). In particular, xanthones have never been reported as HDACis thus far. Both standard HDACis, TSA and SAHA, were selected as positive controls. TSA is widely used as a standard inhibitor for screening HDAC activity, whereas SAHA has already been approved for use as a chemotherapeutic agent (Rajan, Shi, & Xue, 2018). Representative HDACs from class I (HDACs 2 and 8) and class II (HDACs 4 and 7) were chosen as target proteins because they are frequently found at high expression levels in many cancer cell types (Li & Seto, 2016).

The docking energy from the docking program was first determined to predict the binding affinities between the compounds and target proteins. The high docking scores for each compound represent a suitable binding conformation between the compound and protein target. As shown in Table 1, the docking energies of cowaxanthone to HDACs 2, 8, 4 and 7 were high and similar to the standards TSA and SAHA. Interestingly, all values for cowaxanthone are higher than those of both positive controls. This prediction implies that cowaxanthone may be a good HDACi candidate that initially inhibits both classes I and II. To further analyze this role more specifically, as HDACs are metalloenzymes that have zinc ions as cofactors, effective HDACis should interact or chelate this metal ion at the active site.

Figure 2A illustrates the interaction of cowaxanthone with the active site pocket of HDAC2, which was shown in another report as a lipophilic tube connected with the foot pocket. Amino acid residues in the lipophilic tube are GLY154, PHE155, HIS183, PHE210 and LEU276. The foot pocket site contains amino acid residues TYR29, MET35, PHE114 and LEU144. A zinc atom is held by ASP181, HIS183 and ASP269 (Bressi et al., 2010). Herein, our results showed the interaction of cowaxanthone with 13 amino acid residues in the HDAC2 active site, including GLY154, HIS183, PHE210, LEU276, TYR29,

MET 35, LEU 144, HIS 145, HIS 146, GLY142, ARG39, ASP269 and CYS156. Some of these amino acid residues are present in the lipophilic tube and the foot pocket site as previously described. The interaction of cowaxanthone with HIS183 and ASP269 indicates interference with zinc ion binding to the active site. Importantly, the structure of cowaxanthone could directly interact with zinc ions via carbon-hydrogen bonding at ZN379.

The active site of HDAC8 has a characteristic long narrow hydrophobic tunnel that has crucial amino acid residues such as GLY151, PHE152, HIS180, PHE208, MET274 and TRY306 (Vijayakumar, Umamaheswari, Puratchikody, & Velmurugan, 2011). As shown in our work, cowaxanthone interacted with 7 HDAC8 amino acid residues: PHE152, TYR306, TYR111, PRO35, TRP141, PRO273 and ILE34. Importantly, hydrogen bonds were formed with TYR306 and PHE152, which are the key residues in the HDAC8 active site (Figure 2B).

The interactions of cowaxanthone with class II HDAC4 is also demonstrated in Figure 3A. Six amino acid residues of HDAC4 were found to coordinate with cowaxanthone, including HIS158, HIS159, PHE227, PRO155, PRO156, and ARG154. When compared to other works, 3 out of 6 of these residues are exactly the same as those previously described, as shown in the active site of HDAC4, which are HIS159, HIS158 and PRO156 (Berger et al., 2013). In addition, cowaxanthone could interact with zinc ions with a metal-acceptor bond at ZN1411. Moreover, the interactions of cowaxanthone with key amino acid residues, a conventional hydrogen bond with HIS159, a pi-pi T-shaped interaction with HIS198 and an alkyl interaction with PRO156, were established.

For HDAC7, the results illustrated in Figure 3B show that the cowaxanthone ligand could interact with key amino acid residues at the active site of HDAC7, similar to other reports, including a conventional hydrogen bond with GLY678, carbon-hydrogen bonds with HIS709 and PRO809, a pi-anion bond with ASP626, pi-pi stacking with PHE679 and PHE738, a pi-pi T-shaped bond with HIS709 and pi-alkyl bonds with HIS669 and HIS843 (Schuetz et al., 2008). In addition, a carbon-hydrogen bond occurred between cowaxanthone and zinc ion ZN101.

All these data support that cowaxanthone is a promising HDAC inhibitor that interacts with zinc ions and key amino acid residues at the active sites of both class I (HDACs 2 and 8) and class II (HDACs 4 and 7) HDACs. Suppression of HDAC activity is widely recognized as a promising way to reverse aberrant acetylation states that sequentially alter gene expression and induce different phenotypes, such as growth arrest, differentiation and apoptosis (Yelton & Ray, 2018). So, HDACi is recently accepted as a new type of anticancer agent.

Table 1 The docking energies (kcal/mol) of compounds and binding interactions of cowaxanthone in the pocket site of HDAC enzymes

Crystal structure of HDAC enzyme		Docking energy (kcal/mol)		
		SAHA CID: 5311	TSA CID: 444732	Cowaxanthone CID: 10386850
Class I HDACs	HDAC2 (PDB ID: 3MAX)	80.79	92.81	105.56
	HDAC8 (PDB ID: 1T64)	72.61	73.80	74.24
Class II HDACs	HDAC4 (PDB ID: 4VQM)	70.30	79.48	81.00
	HDAC7 (PDB ID: 3C10)	68.57	89.04	92.88

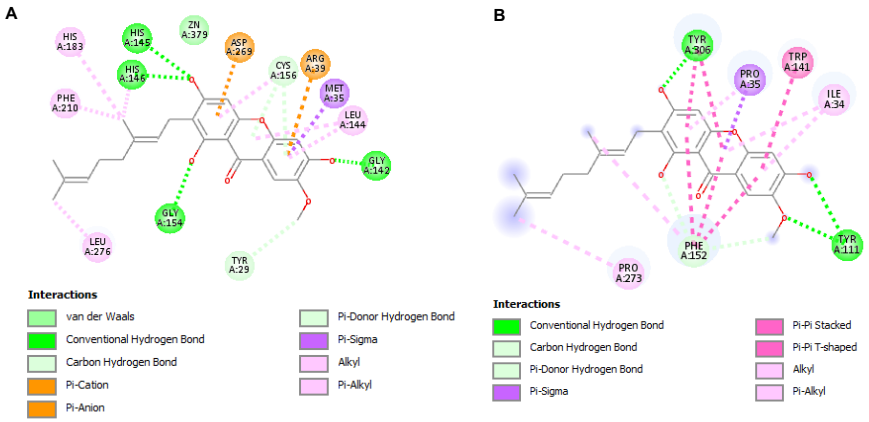

Figure 2 Binding modes of cowaxanthone with the class I HDACs 2 (A) and 8 (B) in a 2D diagram

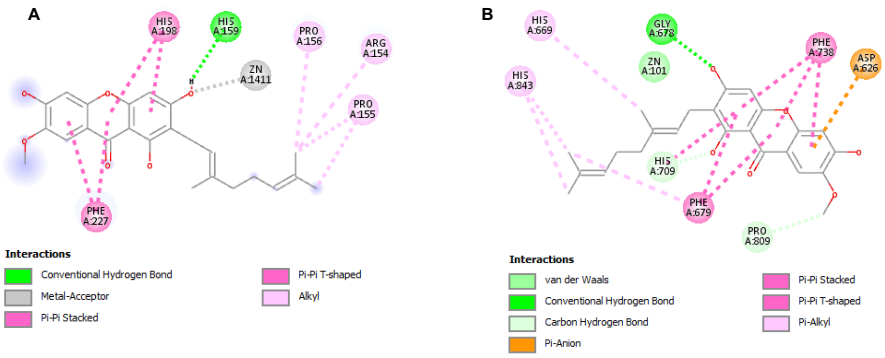

Figure 3 Binding modes of cowaxanthone with the class II HDACs 4 (A) and 7 (B) in a 2D diagram

4.2 HDAC inhibition was confirmed by the *in vitro* screening assay and hyperacetylation of histone proteins

According to the data from computational analysis, cowaxanthone may have a role as an HDACi, so an *in vitro* inhibition assay was carried out. In this method, both TSA and SAHA were used as positive controls, and vehicle 0.5% DMSO was used as a negative control. The results displayed in Table 2 show that cowaxanthone decreased the activity of HDACs in a dose-dependent manner. At 5 µM cowaxanthone, HDAC activity was significantly reduced compared to the negative control (p<0.001). Moreover, cowaxanthone at 100 µM inhibited HDAC by more than 50%, and cowaxanthone at 200 µM inhibited HDAC by approximately 70%. The IC_{50} of cowaxanthone for HDAC inhibition was 68.85 ± 2.94 µM. However, this level of inhibition was less than that of the positive controls TSA and SAHA. Both TSA and SAHA could inhibit HDAC with high potency (more than 70% at 1.25 µM). These data seem to contradict the docking energy results (Table 1) that demonstrated a higher potency of cowaxanthone than the standards TSA and SAHA. These different effects are probably due to several factors. The *in vitro* study performed in the cell lysate contains all isoforms of HDACs, of which about 18 HDACs are found in human cells (Hull, Montgomery, & Leyva, 2016). The docking results were a prediction based on the representative HDACs of class I (HDACs 2 and 8) and II (HDACs 4 and 7). Therefore, the level of inhibition in the *in vitro* situation may differ from the computational study. Additionally, compounds with different structures may have the ability to interact with each HDAC at different levels. However, even cowaxanthone was less effective than the standard HDACi, but HDAC was clearly

inhibited in a dose-dependent manner. In particular, the level of inhibition is much better than that of other known natural HDACis, such as sodium butyrate and valproic acid, which have IC_{50} values of 970 μM and 400 μM, respectively (Phiel et al., 2001; Senawong et al., 2013). To confirm the HDACi role at the molecular level, we performed Western blotting of acetylated histones H3 and H4 in Jurkat cells treated with cowaxanthone at 0, 60, 80 and 100 μM for 12 h. As shown in Figure 4, the hyperacetylation of the histones increased in a dose-dependent manner, confirming the inhibitory effects of cowaxanthone on HDAC. Therefore, we decided to further examine whether cowaxanthone has cancer cytotoxicity.

Table 2 The *in vitro* HDAC inhibitory activity of cowaxanthone. TSA and SAHA (1.25 μM) were used as positive HDAC inhibitors, whereas the vehicle (0.5% DMSO) was used as a negative control. The IC_{50} of cowaxanthone for HDAC inhibition was 68.85 ± 2.94 μM.

Cowaxanthone concentration (μM)	HDAC inhibition (%)
0 (vehicle)	0.00 ± 0.00
5	21.30 ± 4.20
25	32.39 ± 3.76
50	43.01 ± 2.70
100	57.15 ± 3.05
200	66.97 ± 1.70
SAHA	70.93 ± 1.68
TSA	97.73 ± 1.58

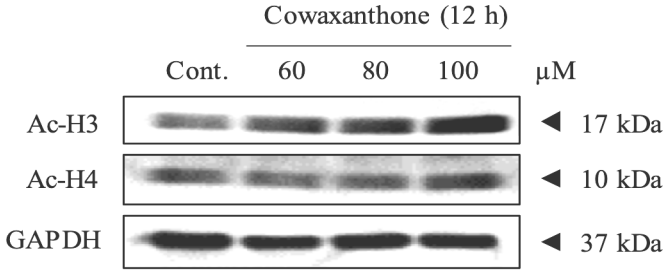

Figure 4 Western blot analysis of acetylated H3 and H4 in Jurkat cells. Jurkat cells were treated with cowaxanthone at 0, 60, 80 and 100 μM for 12 h. GAPDH; Glyceraldehyde-3-phosphate dehydrogenase was used as a loading control.

4.3 Cowaxanthone is cytotoxic to different types of cancer cells

In order to investigate the cytotoxic effects of cowaxanthone in cancer cells, an MTT assay was performed. Due to most of cancer cells are highly expressed in HDACs (Li & Seto, 2016). Jurkat and MDA-MB-231 cells were selected as representative cancer cells, which are hematological and solid tumor types, respectively. The cytotoxicity was compared with Vero cells, a commonly used normal cell line for cytotoxic evaluation. In addition, we conducted a parallel experiment with SAHA to compare the level of toxicity with that of cowaxanthone. SAHA was selected instead of TSA, as SAHA has already been approved for clinical use. Therefore, we postulated that if cowaxanthone has a level of toxicity that is comparable to SAHA, this result should imply the potential effect of cowaxanthone as an anticancer agent. As shown in Figure 5, the MTT assay revealed that cowaxanthone significantly inhibited cell viability in a dose-dependent manner in both Jurkat and MDA-MB-231 cells, with IC_{50} values of 88.50 ± 6.20 and 96.05 ± 2.55 μM, respectively. The effect on Vero cells was less pronounced with an IC_{50} of 110.40 ± 6.13 μM. These data reveal that cowaxanthone is a good anticancer agent because it is less toxic to normal cells. SAHA also displayed cytotoxicity with selectively to only Jurkat cells (Table 3). However, this cytotoxic is less effective

than cowaxanthone about three-fold, indicating better cytotoxicity of cowaxanthone. Additionally, the level of cancer cytotoxicity of cowaxanthone was in a similar range to that of other HDACis. For example, the cytotoxic effects of kaempferol, a preclinical HDACi, against HepG2 cells was 84.72 ± 8.53 μM (Dashwood, Myzak, & Ho, 2006). Thus, these data support the potential of cowaxanthone as a good candidate anticancer agent, not only demonstrating its role as an HDACi but also clearly specifying a cytotoxic effect on cancer cells. More importantly, this cytotoxicity is less pronounced in normal cells.

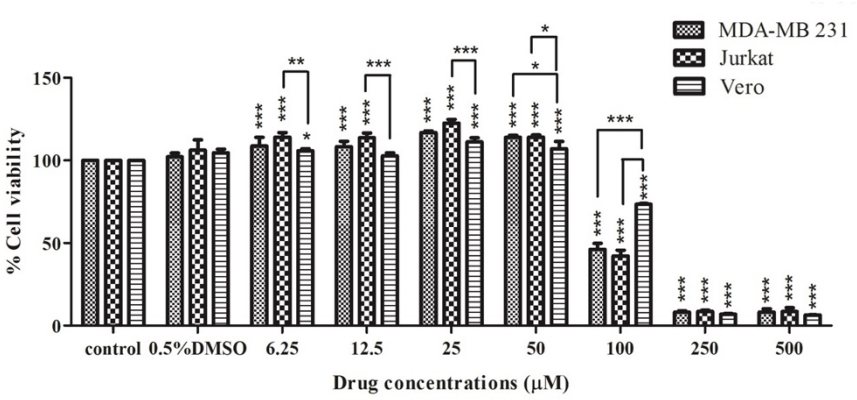

Figure 5 Cytotoxicity of cowaxanthone in different cell lines. Jurkat, MDA-MB-231 and Vero cells were treated with different concentrations of cowaxanthone (0-100 μM) for 24 h, whereas 0.5% DMSO served as the negative control. The MTT assay was performed following a standard method. The percent cell viability is presented as the mean ± SD in triplicate (n=3). *p<0.05, **p<0.01 ***p<0.001 versus untreated cells.

Table 3 IC_{50} of cowaxanthone and SAHA in different cell lines

Compounds	Cell lines (IC50; μM)		
	Jurkat	MDA-MB-231	Vero
cowaxanthone	88.50 ± 2.89	96.05 ± 2.55	110.40 ± 6.13
SAHA	273.23 ± 5.20	> 500	> 500

4.4 An apoptotic mechanism is induced by cowaxanthone

Apoptosis induction is recognized as an important target mechanism of various anticancer agents, including HDACis (Hassan, Watari, AbuAlmaaty, Ohba, & Sakuragi, 2014). This is because this process is not harmful to patients and does not induce an inflammatory response. Therefore, it is interesting to investigate whether cowaxanthone induces cancer cell death by an apoptotic mechanism. Jurkat cells were selected as a model of study, as better cytotoxic effects were obtained compared to MDA-MB-231 cells. The well-known characteristics of apoptotic cells were evaluated, such as cell shrinkage, nuclear condensation and fragmentation, and apoptotic body formation. As demonstrated in Figure 6, cowaxanthone could induce all the basic characteristics of apoptosis. DNA fragmentation and apoptotic body formation were clearly observed after 24 h of treatment with 60 μM cowaxanthone. To provide stronger evidence, we performed Western blotting of caspase-3, caspase-8 and caspase-9, which are major mediators of apoptotic signaling. As shown in Figure 7, the cleavage forms of all caspases are clearly depicted. These data are consistent with other xanthone reports. For example, α-mangostin induces apoptosis in SW1353 cells by causing DNA fragmentation, activation of caspase-3, caspase-8, and caspase-9, and the release of cytochrome c from the mitochondria (Krajarng, Nakamura, Suksamrarn, & Watanapokasin, 2011). Moreover, α-mangostin activates mitochondrial dysfunction and mediates apoptosis through the activation of caspase-9 and caspase-3 in human promyelocytic leukemia (HL-

60) cells (Matsumoto et al., 2004). Additionally, apoptosis induction is recognized as the prominent route of HDACi action (Ma et al., 2015). Altogether, our data confirmed the potential function of cowaxanthone as an HDACi that is sequentially cytotoxic to cancer cells and induces cell death by an apoptotic mechanism.

.

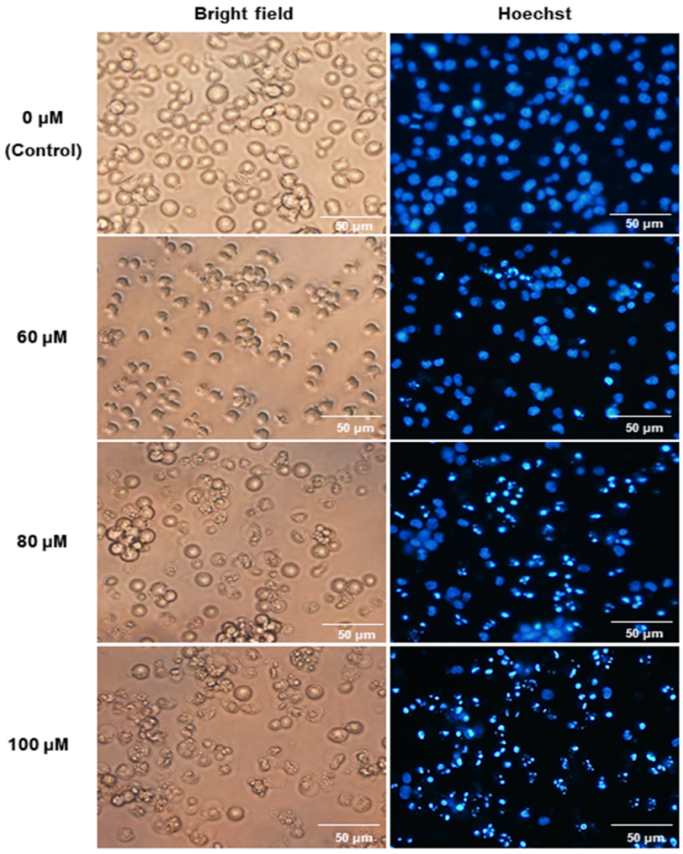

Figure 6 Apoptotic nuclear morphology induced by cowaxanthone. Cells were treated with 0, 60, 80 and 100 μM cowaxanthone for 24 h and then stained with Hoechst 33342 at a final concentration of 5 μg/mL. Then, the cells were observed with a fluorescence microscope (magnification, ×50). Bright field (left) and fluorescent dye Hoechst 33342 (right) are shown.

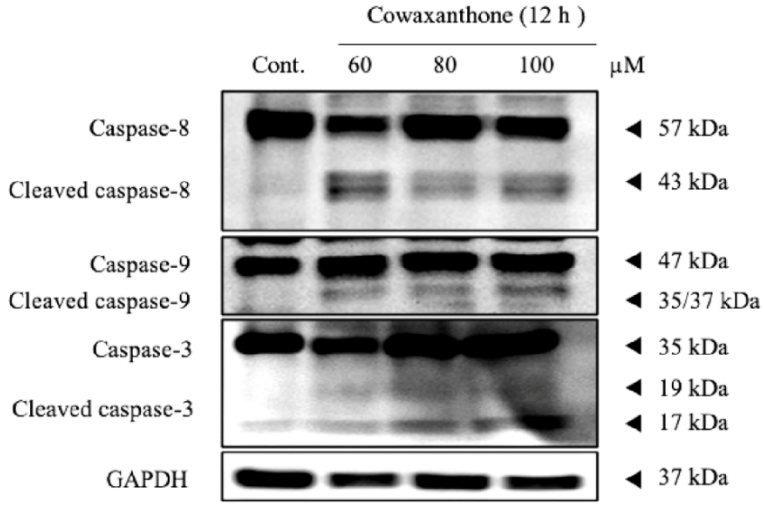

Figure 7 Western blot analysis of caspases in Jurkat cells. Cells were treated with cowaxanthone at 0, 60, 80 and 100 μM for 12 h. Glyceraldehyde-3-phosphate dehydrogenase (GAPDH) was used as a loading control.

5. Conclusion

The present study demonstrated for the first time that a natural xanthone, cowaxanthone, has the ability to be a good therapeutic agent for cancer treatment. It can act as both class I and II HDAC inhibitor as demonstrated by *in silico* docking, an *in vitro* study and the level of histone hyperacetylation. Additionally, cowaxanthone exhibits cytotoxicity to leukemic T cells and breast cancer cells but is less cytotoxic to normal cells. The mode of cell death induced by cowaxanthone was clearly identified as apoptosis, which is an accepted target of potential anticancer drugs. Further investigations on the mechanism of cancer cell growth suppression and evaluations of the efficacy of cowaxanthone in an *in vivo* model should be evaluated.

6. Acknowledgments

This work was financially supported by the grants from the Capacity Building Program for New Research 2018 (Grant No. D08-61), the national Research Council of Thailand (NRCT), Faculty of Medicine (Grant No.376/2558, 143/2561), Graduate School and Strategic Wisdom and Research Institute of Srinakharinwirot University. We are thankful to the Center of Excellence for Innovation in Chemistry (PERCH-CIC), Ministry of Higher Education, Science, Research and Innovation and the Department of Chemistry, Faculty of Science, Srinakharinwirot University for support.

7. References

Berger, A., Venturelli, S., Kallnischkies, M., Bocker, A., Busch, C., Weiland, T., Noor, S., Leischner, C., Weiss, T. S., Lauer, U. M., Bischoff, S. C., & Bitzer, M. (2013). Kaempferol, a new nutrition-derived pan-inhibitor of human histone deacetylases. *Journal of Nutritional Biochemistry, 24*(6), 977-985. DOI: 10.1016/j.jnutbio.2012.07.001

Bressi, J. C., Jennings, A. J., Skene, R., Wu, Y., Melkus, R., De Jong, R., O'Connell, S., Grimshaw, C. E., Navre, M., & Gangloff, A. R. (2010). Exploration of the HDAC2 foot pocket: synthesis and SAR of substituted N-(2-aminophenyl)benzamides. *Bioorganic & Medicinal Chemistry Letters, 20*(10), 3142-3145. DOI: 10.1016/j.bmcl.2010.03.091

Dashwood, R. H., Myzak, M. C., & Ho, E. (2006). Dietary HDAC inhibitors: time to rethink weak ligands in cancer chemoprevention? *Carcinogenesis, 27*(2), 344-349. DOI: 10.1093/carcin/bgi253

de Ruijter, A. J. M., van Gennip, A. H., Caron, H. N., Kemp, S., & van Kuilenburg, A. B. (2003). Histone deacetylases (HDACs): characterization of the classical HDAC family. *Biochemical Jpurnal, 370*(3), 737-749. DOI: 10.1042/BJ20021321

Ha, L. D., Hansen, P. E., Vang, O., Duus, F., Pham, H. D., & Nguyen, L. H. (2009). Cytotoxic geranylated xanthones and O-alkylated derivatives of alpha-mangostin. *Chemical & Pharmaceutical Bulletin (Tokyo), 57*(8), 830-834. DOI: 10.1248/cpb.57.830

Hassan, M., Watari, H., AbuAlmaaty, A., Ohba, Y., & Sakuragi, N. (2014). Apoptosis and molecular targeting therapy in cancer. *BioMed Research International, 2014*, 150845. DOI: 10.1155/2014/150845

Hull, E. E., Montgomery, M. R., & Leyva, K. J. (2016). HDAC inhibitors as epigenetic regulators of the immune system: impacts on cancer therapy and inflammatory diseases. *BioMed Research International, 2016*, ID 8797206. DOI: 10.1155/2016/8797206

Jan, R., & Chaudhry, G. E. (2019). Understanding apoptosis and apoptotic pathways targeted cancer therapeutics. *Advanced Pharmaceutical Bulletin, 9*(2), 205-218. DOI: 10.15171/apb.2019.024

Krajarng, A., Nakamura, Y., Suksamrarn, S., & Watanapokasin, R. (2011). Alpha-mangostin induces apoptosis in human chondrosarcoma cells through downregulation of ERK/JNK and Akt signaling pathway. *Journal of Agricultural and Food Chemistry, 59*(10), 5746-5754. DOI: 10.1021/jf200620n

Li, Y., & Seto, E. (2016). HDACs and HDAC inhibitors in cancer development and therapy. *Cold Spring Harbor Perspectives in Medicine, 6*(10), a026831. DOI: 10.1101/cshperspect.a026831

Ma, J., Guo, X., Zhang, S., Liu, H., Lu, J., Dong, Z., Liu, K., & Ming, L. (2015). Trichostatin A, a histone deacetylase inhibitor, suppresses proliferation and promotes apoptosis of esophageal squamous cell lines. *Molecular Medicine Reports, 11*(6), 4525-4531. DOI:10.3892/mmr.2015.3268

Matsumoto, K., Akao, Y., Yi, H., Ohguchi, K., Ito, T., Tanaka, T., Kobayashi, E., Iinumac, M., & Nozawa, Y. (2004). Preferential target is mitochondria in alpha-mangostin-induced apoptosis in human leukemia HL60 cells. *Bioorganic & Medicinal Chemistry, 12*(22), 5799-5806. DOI: 10.1016/j.bmc.2004.08.034

Negi, J. S., Bisht, V. K., Singh, P., Rawat, M. S. M., & Joshi, G. P. (2013). Naturally occurring xanthones: chemistry and biology. *Journal of Applied Chemistry, 2013*, 621459. DOI: 10.1155/2013/621459

Nguyen, N. K., Truong, X. A., Bui, T. Q., Bui, D. N., Nguyen, H. X., Tran, P. T., & Nguyen, L. D. (2017). Alpha-glucosidase inhibitory xanthones from the roots of *Garcinia fusca*. *Chemistry & Biodiversity, 14*(10). DOI: 10.1002/cbdv.201700232

Nontakham, J., Charoenram, N., Upamai, W., Taweechotipatr, M., & Suksamrarn, S. (2014). Anti-helicobacter pylori xanthones of *Garcinia fusca*. *Archives of Pharmacal Research volume, 37*(8), 972-977. DOI: 10.1007/s12272-013-0266-4

Phiel, C. J., Zhang, F., Huang, E. Y., Guenther, M. G., Lazar, M. A., & Klein, P. S. (2001). Histone deacetylase is a direct target of valproic acid, a potent anticonvulsant, mood stabilizer, and teratogen. *The Journal of Biological Chemistry, 276*(39), 36734-36741. DOI: 10.1074/jbc.M101287200

Rajan, A., Shi, H., & Xue, B. (2018). Class I and II histone deacetylase inhibitors differentially regulate thermogenic gene expression in brown adipocytes. *Scientific Reports, 8*(1), 13072. DOI: 10.1038/s41598-018-31560-w

Schuetz, A., Min, J., Allali-Hassani, A., Schapira, M., Shuen, M., Loppnau, P., Mazitschek, R., Kwiatkowski, N. P., Lewis, T. A., Maglathin, R. L., McLean, T. H., Bochkarev, A., Plotnikov, A. N., Vedadi, M., & Arrowsmith, C. H. (2008). Human HDAC7 harbors a class IIa histone deacetylase-specific zinc binding motif and cryptic deacetylase activity. *Journal of Biological Chemistry, 283*(17), 11355-11363. DOI: 10.1074/jbc.M707362200

Senawong, T., Misuna, S., Khaopha, S., Nuchadomrong, S., Sawatsitang, P., Phaosiri, C., Surapaitoon, A., & Sripa, B. (2013). Histone deacetylase (HDAC) inhibitory and antiproliferative activities of phenolic-rich extracts derived from the

rhizome of Hydnophytum formicarum Jack.: sinapinic acid acts as HDAC inhibitor. *BMC Complementary Medicine and Therapies, 13*, 232. DOI: 10.1186/1472-6882-13-232

Singh, A. K., Bishayee, A., & Pandey, A. K. (2018). Targeting histone deacetylases with natural and synthetic agents: An emerging anticancer strategy. *Nutrients, 10*(6), 731 DOI: 10.3390/nu10060731

Vijayakumar, B., Umamaheswari, A., Puratchikody, A., & Velmurugan, D. (2011). Selection of an improved HDAC8 inhibitor through structure-based drug design. *Bioinformation, 7*(3), 134-141. DOI: 10.6026/97320630007134

Yelton, C. J., & Ray, S. K. (2018). Histone deacetylase enzymes and selective histone deacetylase inhibitors for antitumor effects and enhancement of antitumor immunity in glioblastoma. *Neuroimmunology and neuroinflammation, 5*, 46. DOI: 10.20517/2347-8659.2018.58

Yoon, S., & Eom, G. H. (2016). HDAC and HDAC Inhibitor: from cancer to cardiovascular diseases. *Chonnam medical journal, 52*(1), 1-11. DOI: 10.4068/cmj.2016.52.1.1

Zhang, J., & Zhong, Q. (2014). Histone deacetylase inhibitors and cell death. *Cellular and Molecular Life Sciences volume, 71*(20), 3885-3901. DOI: 10.1007/s00018-014-1656-6